



Density-matrix functional theory of the attractive Hubbard model: Statistical analogy of pairing correlations

T. S. Müller and G. M. Pastor *Institut für Theoretische Physik, Universität Kassel, Heinrich-Plett-Strasse 40, 34132 Kassel, Germany* (Received 15 October 2021; revised 8 December 2022; accepted 20 December 2022; published 29 December 2022)

The ground-state properties of the Hubbard model with attractive local pairing interactions are investigated in the framework of lattice density-functional theory. A remarkable correlation is revealed between the interaction-energy functional $W[\eta]$ corresponding to the Bloch-state occupation-number distribution $\eta_{k\sigma}$ and the entropy $S[\eta]$ of a system of noninteracting fermions having the same $\eta_{k\sigma}$. The relation between $W[\eta]$ and $S[\eta]$ is shown to be approximately linear for a wide range of ground-state representable occupation-number distributions $\eta_{k\sigma}$. Taking advantage of this statistical analogy, a simple explicit ansatz for $W[\eta]$ of the attractive Hubbard model is proposed, which can be applied to arbitrary periodic systems. The accuracy of this approximation is demonstrated by calculating the main ground-state properties of the model on several 1D and 2D bipartite and nonbipartite lattices and by comparing the results with exact diagonalizations.

DOI: [10.1103/PhysRevB.106.245148](https://doi.org/10.1103/PhysRevB.106.245148)

I. INTRODUCTION

The study of strongly correlated phenomena in quantum many-body systems is one of the central challenges in condensed-matter physics. Over the past decades, the field has experienced a remarkable expansion which has been fueled by the discovery of new materials, as well as by the progress in experimental characterization tools and theoretical methodologies. One of the most significant developments in this field has been the discovery of high-temperature superconductors and the electronic pairing mechanism associated with them [1,2]. Indeed, in these materials the origin of superconductivity is profoundly different from the phonon-mediated coupling at the center of the Bardeen, Cooper, and Schrieffer (BCS) theory of conventional superconductors [3]. As a result, the study of alternative descriptions of pairing interactions in solids have gained increasing attention [1,4–10].

The attractive single-band Hubbard model [11–13] with on-site interactions $U < 0$ provides a simple, albeit oversimplified way of introducing a pairing mechanism among fermions and of exploring its consequences on the many-body properties [14–18]. Originally proposed for describing local repulsive Coulomb interactions in the context of itinerant narrow-band magnetism [11–13], this model has played, together with other lattice models [19–21], a most significant role in shaping our understanding of strongly correlated phenomena. Therefore, it is most interesting to explore its physical properties when pairing is favored. From this perspective, it is important to recall that the physics described by the attractive Hubbard model is intrinsically different from the pairing mechanism of the BCS theory. The effective interactions in the BCS theory have an off-diagonal character since they are mediated by electron-phonon scattering. Moreover, the narrow energy and momentum dispersion caused by the interaction with phonons results in a large spatial extension

of the Cooper pairs. In contrast, the pairing interactions are strictly local in the Hubbard model, since they only affect fermions occupying the same lattice site. Rather than a limitation, this strong complementarity is one of the reasons why the model is particularly appealing from a theoretical perspective [22].

Local attractive interactions have been the subject of multiple theoretical studies by using a variety of methodologies [14–18,22–31]. In early works, the formation and stability of charge-density waves and superconducting states has been quantified [14,15]. In addition, the phase diagram of the two-dimensional (2D) negative- U Hubbard model has been determined [16,17]. Other investigations have addressed the accuracy of the mean-field BCS approximation by comparing it with the exact Bethe-ansatz solution of the one dimensional (1D) Hubbard model as well as with accurate numerical calculations in two dimensions [23–26]. More recently, the model has been studied in the framework of lattice density-functional theory (LDFT) [18] by applying the concepts of first-principles density-functional theory (DFT) [32,33] to many-body lattice Hamiltonians. An explicit semilocal approximation to the interaction energy W has been proposed as a functional of the single-particle density matrix (SPDM) γ . In this way, the ground-state kinetic, Coulomb, and total energies, the charge distribution, and nearest-neighbor (NN) bond order as well as the pairing energy have been determined for various 1D, 2D, and 3D lattices [18]. Moreover, even-odd and supereven oscillations of the pairing energy have been observed as a function of the band filling in agreement with previous studies [24].

The purpose of this paper is to investigate the properties of the attractive Hubbard model in the framework of LDFT. As a complement to previous studies [18], which are based on the exact solution of the two-site problem and the scaling properties of $W[\gamma]$, we adopt here a delocalized k -space

perspective. Thus, the translational symmetry of the lattice allows us to regard the interaction energy W as a functional of the occupation-number distribution $\eta_{k\sigma}$ of the Bloch states having wave vector \mathbf{k} . As in any density-functional approach, the accuracy of the outcome relies on the quality of the considered approximation to the functional $W[\eta]$, where η denotes the vector with components $\eta_{k\sigma}$. Therefore, our first goal is to propose an appropriate explicit ansatz for $W[\eta]$, which in our case is based on a statistical interpretation of pairing correlation effects. An analogous approach has been recently proven to be quite successful for repulsive interactions [34]. Once the functional is introduced and its capacity to correctly describe attractive interactions is examined, we proceed to a number of applications of LDFT to 1D and 2D negative- U Hubbard models to assess the quantitative accuracy of the method and to discuss its goals and limitations.

The remainder of the paper is organized as follows. In Sec. II, the main concepts of LDFT are recalled. This includes discussing the central role played by the SPDM $\boldsymbol{\gamma}$ and the Bloch-state occupation-number distribution $\eta_{k\sigma}$, as well as introducing the variational principle from which the ground-state properties are derived. In Sec. III, a remarkable correlation is revealed between the interaction energy W of the attractive Hubbard model and the entropy S of a system of noninteracting fermions, both regarded as functionals of $\eta_{k\sigma}$. Based on this statistical analogy, we formulate the so-called independent-fermion entropy (IFE) approximation to the interaction-energy functional $W[\eta]$. Applications of this ansatz to the attractive Hubbard model on 1D and 2D lattices are presented and discussed in Sec. IV. Comparison with exact numerical calculations underscores the accuracy and predictive power of the method. Finally, the paper is closed in Sec. V with a summary of our conclusions.

II. THEORETICAL BACKGROUND

Consider a many-body lattice Hamiltonian consisting of a single-particle kinetic energy operator \hat{T} and a two-particle interaction operator \hat{W} ,

$$\hat{H} = \hat{T} + \hat{W} = \sum_{ij\sigma} t_{ij\sigma} \hat{c}_{i\sigma}^\dagger \hat{c}_{j\sigma} + \frac{1}{2} \sum_{\substack{ijkl \\ \sigma\sigma'}} W_{ijkl}^{\sigma\sigma'} \hat{c}_{i\sigma}^\dagger \hat{c}_{j\sigma'}^\dagger \hat{c}_{l\sigma} \hat{c}_{k\sigma}, \quad (1)$$

where $\hat{c}_{i\sigma}^\dagger$ ($\hat{c}_{i\sigma}$) creates (annihilates) an electron with spin σ in the orbital $\phi_i(\mathbf{r})$. In the case of single-band models as the Hubbard model, the index i corresponds simply to the lattice site, while in multiband models (e.g., d -band models) it also labels the different local orbitals which are taken into account. The parameters in \hat{H} are the single-particle energy levels $t_{i\sigma}$ and hopping integrals $t_{ij\sigma}$ with $i \neq j$, which define \hat{T} , and the interaction integrals $W_{ijkl}^{\sigma\sigma'}$, which define \hat{W} . Once the orbitals and basic characteristics of the model interactions $W_{ijkl}^{\sigma\sigma'}$ are adopted, the problem is entirely set by the the single-particle matrix elements $t_{ij\sigma}$. In particular they define the dimensionality and topology of the lattice, the range of the single-particle hybridizations, and the relative importance between kinetic and interaction energies which conditions the nature of the correlations.

Since the hoppings $t_{ij\sigma}$ enter the Hamiltonian in a bilinear form together with the operators $\hat{c}_{i\sigma}^\dagger \hat{c}_{j\sigma}$, it is possible to replace the wave function $|\Psi\rangle$ or the mixed-state density-matrix $\hat{\rho}$ by the SPDM $\boldsymbol{\gamma}$, whose elements are $\gamma_{ij\sigma} = \langle \hat{c}_{i\sigma}^\dagger \hat{c}_{j\sigma} \rangle$, as the central unknown of the many-body problem [35,36]. The situation is analogous to the one found in the first-principles theory of the inhomogeneous electron gas, where the external potential $v(\mathbf{r})$ defines the problem and therefore the electronic density $\rho(\mathbf{r})$ becomes the central variable of DFT [32]. A proof of the Hohenberg-Kohn theorem for lattice models may be found in Ref. [37].

Starting from the ground-state variational principle and following Levy and Lieb's two-step minimization [38,39], it is easy to show that the ground-state energy of the many-body Hamiltonian \hat{H} is given by

$$E_0 = \min_{\boldsymbol{\gamma} \in \Gamma_N} \left\{ \sum_{ij\sigma} t_{ij\sigma} \gamma_{ij\sigma} + W[\boldsymbol{\gamma}] \right\}, \quad (2)$$

where the minimization runs over the set Γ_N of all physical single-particle density matrices, i.e., over all $\boldsymbol{\gamma}$ which can be obtained from an N -particle wave function $|\Psi\rangle$ or a mixed state $\hat{\rho}$. The interaction energy $W[\boldsymbol{\gamma}]$ is a universal functional of $\boldsymbol{\gamma}$, i.e., a functional which is independent of the hopping integrals defining the specific problem under consideration. Of course, $W[\boldsymbol{\gamma}]$ depends on the form and nature of the interactions $W_{ijkl}^{\sigma\sigma'}$ and on the number of particles N which is given by $\boldsymbol{\gamma}$ itself ($N = \sum_{i\sigma} \gamma_{ii\sigma}$). Physically, $W[\boldsymbol{\gamma}]$ represents the minimum value that the interaction energy of the many-body system can take when the SPDM is equal to $\boldsymbol{\gamma}$. This can be clearly seen from its formal expression [35,37,40,41]

$$W[\boldsymbol{\gamma}] = \min_{\hat{\rho} \rightarrow \boldsymbol{\gamma}} \text{Tr}\{\hat{\rho} \hat{W}\}, \quad (3)$$

where the minimization runs over all N -particle mixed states $\hat{\rho}$ yielding $\langle \hat{c}_{i\sigma}^\dagger \hat{c}_{j\sigma} \rangle = \gamma_{ij\sigma}$ for all $ij\sigma$. While the physical interpretation of $W[\boldsymbol{\gamma}]$ is transparent and sound, particularly in combination with Eq. (2), finding its exact functional dependence is far from simple, since $W[\boldsymbol{\gamma}]$ conceals, among other information, the interaction energy in the ground state of \hat{H} for all possible band fillings and hopping integrals $t_{ij\sigma}$ [42]. As in the theory of the inhomogeneous electron gas, the challenge in LDFT is to find accurate explicit approximations to $W[\boldsymbol{\gamma}]$. Once such an approximation is available, Eq. (2) implies that the ground-state energy and density matrix can be obtained by minimizing the energy functional

$$E[\boldsymbol{\gamma}] = T[\boldsymbol{\gamma}] + W[\boldsymbol{\gamma}] = \sum_{ij\sigma} t_{ij\sigma} \gamma_{ij\sigma} + W[\boldsymbol{\gamma}] \quad (4)$$

with respect to $\boldsymbol{\gamma}$, which can thus be regarded as the central variable of the many-body problem [35,36].

In periodic solids, it is meaningful to take advantage of translational symmetry and restrict the domain of minimization to translational invariant density matrices. In this case

$$\gamma_{ij\sigma} = \sum_{\mathbf{k}} u_{i\mathbf{k}\sigma} \eta_{\mathbf{k}\sigma} u_{j\mathbf{k}\sigma}^*, \quad (5)$$

where the eigenvectors $\mathbf{u}_{\mathbf{k}\sigma}$ of $\boldsymbol{\gamma}$ are Bloch states and the eigenvalues $\eta_{\mathbf{k}\sigma}$ represent the corresponding occupation numbers. Note that in single-band models \mathbf{k} stands simply for

the Bloch wave-vector in the first Brillouin zone, whereas in multiband models it also implicitly includes the band index. In the former case (one orbital per unit cell), the eigenvectors are entirely defined by translational symmetry and can thus be classified by the Bloch wave-vector \mathbf{k} . This represents a significant simplification which applies, in particular, to the Hubbard model. It means that the kinetic and interaction energy can be regarded as functionals $T[\boldsymbol{\eta}]$ and $W[\boldsymbol{\eta}]$ of the occupation number distribution $\eta_{\mathbf{k}\sigma}$ alone. Only in the single-band case the shape of the ground-state density-matrix eigenvectors can be assumed to be independent of the parameters defining the physical model (e.g., band filling, interaction strength, etc.).

III. STATISTICAL ANALOGY

To develop an explicit practical approximation to the interaction-energy functional $W[\boldsymbol{\eta}]$, we focus on the attractive single-band Hubbard model

$$\hat{H} = \hat{T} + \hat{W} = \sum_{ij\sigma} t_{ij} \hat{c}_{i\sigma}^\dagger \hat{c}_{j\sigma} + U \sum_i \hat{n}_{i\uparrow} \hat{n}_{i\downarrow}, \quad (6)$$

where t_{ij} stands for the hopping integral between sites i and j , $U \leq 0$ is the local interaction strength, and $\hat{n}_{i\sigma} = \hat{c}_{i\sigma}^\dagger \hat{c}_{i\sigma}$ is the number operator for spin σ at site i . Consequently, the interaction-energy functional according to Eq. (3) is given by

$$W[\boldsymbol{\gamma}] = \min_{\hat{\rho} \rightarrow \boldsymbol{\gamma}} \left\{ U \sum_i \langle \hat{n}_{i\uparrow} \hat{n}_{i\downarrow} \rangle \right\} = U \max_{\hat{\rho} \rightarrow \boldsymbol{\gamma}} \left\{ \sum_i \langle \hat{n}_{i\uparrow} \hat{n}_{i\downarrow} \rangle \right\}, \quad (7)$$

where we have used that $U \leq 0$. Two important limiting cases, for which Levy's constrained minimization in Eq. (7) can be exactly solved, are worth considering from the start. The first one is the scalar spin-density matrix $\gamma_{ij\sigma} = \delta_{ij} n_\sigma$, where the density $n_\sigma = N_\sigma / N_a$ and total number N_σ of spin- σ fermions are the same for both spins and N_a denotes the number of atoms. The corresponding occupation numbers $\eta_{\mathbf{k}\sigma} = n_\sigma$ are then independent of \mathbf{k} and σ . In this case, the interaction energy $W[\boldsymbol{\eta}]$ assumes its minimal value $W_\infty = U D_\infty$ by adopting a fully localized state with the maximum number of pairs or double occupations $D_\infty = N_\uparrow = N_\downarrow$. The second important limit is defined by the idempotent density matrices $\boldsymbol{\gamma} = \boldsymbol{\gamma}^2$, which have $\eta_{\mathbf{k}\sigma} = 0$ or 1 for all $\mathbf{k}\sigma$ ($\sum_{\mathbf{k}\sigma} \eta_{\mathbf{k}\sigma} = N_\sigma$). The many-particle states by which idempotent SPDMS can be represented are the Slater determinants made of the Bloch states having $\eta_{\mathbf{k}\sigma} = 1$. The corresponding interaction-energy W is then given by the Hartree-Fock (HF) energy

$$W_{\text{HF}} = U \sum_i \gamma_{i\uparrow} \gamma_{i\downarrow} = U N_a n_\uparrow n_\downarrow, \quad (8)$$

where we have used that $\gamma_{i\sigma} = n_\sigma$ for all i . In this context, it is useful to draw the following statistical analogy by regarding $\eta_{\mathbf{k}\sigma}$ as the average occupation numbers of N_\uparrow and N_\downarrow fermions which are statistically distributed over all the Slater determinants that can be constructed with the single-particle Bloch states [34,43]. In the fully localized state, where pairing is maximal, $\eta_{\mathbf{k}\sigma} = n_\sigma$ is uniform and therefore all Bloch states are equally probable. The occupation-number distribution $\eta_{\mathbf{k}\sigma}$ conceals no *a priori* information on which Bloch states are

occupied and which are empty. The information content of this distribution is zero and the entropy is maximal. On the other extreme, for an idempotent $\boldsymbol{\gamma}$, $\eta_{\mathbf{k}\sigma}$ is equal to 0 or 1, which means that only one Slater determinant is possible. Our knowledge on the distribution of the system across its Slater determinants is complete and the entropy vanishes [34,43]. This suggests that the entropy

$$S[\boldsymbol{\eta}] = - \sum_{\mathbf{k}\sigma} [\eta_{\mathbf{k}\sigma} \ln(\eta_{\mathbf{k}\sigma}) + (1 - \eta_{\mathbf{k}\sigma}) \ln(1 - \eta_{\mathbf{k}\sigma})] \quad (9)$$

of a system of independent fermions having the occupation-number distribution $\eta_{\mathbf{k}\sigma}$ can be regarded as a measure of the ability of the system to minimize the interaction energy under the constraint of the given $\eta_{\mathbf{k}\sigma}$ [see Eq. (7)]. Notice that the IFE assumes its extremes for the same $\eta_{\mathbf{k}\sigma}$ as the interaction energy W : If the fermions are uncorrelated ($\eta_{\mathbf{k}\sigma} = 0$ or 1), $W = W_{\text{HF}}$ is maximal and $S = 0$ is minimal. On the other hand, if the fermions are fully paired and localized ($\eta_{\mathbf{k}\sigma} = n_\sigma$ for all \mathbf{k}), $W = W_\infty = U N_\uparrow = U N_\downarrow$ is minimal and

$$S = S_\infty = -N_a \sum_\sigma [n_\sigma \ln(n_\sigma) + (1 - n_\sigma) \ln(1 - n_\sigma)] \quad (10)$$

is maximal. These correlations suggest that $S[\boldsymbol{\eta}]$, which is itself a functional of the occupation-number distribution $\boldsymbol{\eta}$, can be used for deriving an effective approximation of $W[\boldsymbol{\eta}]$ [34,43,44].

To quantify the actual correlation between $S[\boldsymbol{\eta}]$ and $W[\boldsymbol{\eta}]$, we have performed exact numerical Lanczos diagonalizations of the ground state of the attractive Hubbard model for a number of different lattice structures and band fillings. A wide variety of occupation-number distributions $\boldsymbol{\eta}$ has been explored by varying the hopping integrals from $t_{ij} = 0$ to $|t_{ij}| \gg |U|$ so as to scan $S[\boldsymbol{\eta}]$ in its complete range ($0 \leq S \leq S_\infty$) and by considering different ratios and relative signs between first- and second-NN hoppings. The results shown in Fig. 1 reveal a remarkable nearly one-to-one correspondence between $W[\boldsymbol{\eta}]$ and $S[\boldsymbol{\eta}]$ in all considered situations including bipartite and nonbipartite 1D and 2D lattices, as well as systems having competing first- and second-NN hoppings with unusual single-particle dispersion relations. Moreover, once properly scaled ($W_\infty \leq W \leq W_{\text{HF}}$ and $0 \leq S \leq S_\infty$), the relation becomes approximately independent of the size and dimension of the system under consideration. This pseudouniversal relation between W and S provides an ideal ground for broadly applicable approximations to the interaction-energy functional $W[\boldsymbol{\eta}]$. On the basis of the numerical results shown in Fig. 1, we propose the linear ansatz

$$W[\boldsymbol{\eta}] = W_{\text{HF}} + (W_\infty - W_{\text{HF}}) \frac{S[\boldsymbol{\eta}]}{S_\infty} \quad (11)$$

for the interaction-energy functional of the attractive Hubbard model with $N_\uparrow = N_\downarrow$ fermions. An analogous approximation has already been proposed for the repulsive Hubbard model at half-band filling ($N_\uparrow + N_\downarrow = N_a$) [34]. A different proportionality relation between the correlation energy and the information entropy of the distribution of occupation numbers $\eta_{\mathbf{k}}$ has been previously proposed by Collins [43] and more recently applied by other authors [45,46] in atomic and molecular calculations [44].

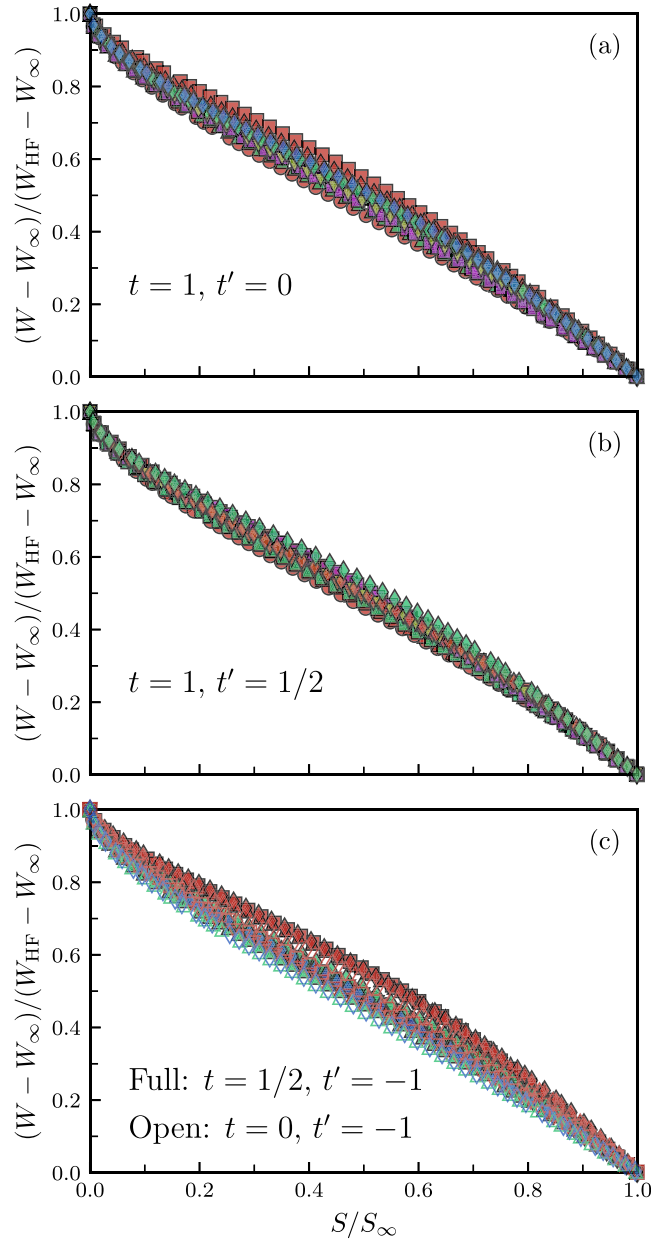


FIG. 1. Correlation between the interaction energy W [Eq. (7)] and the independent-fermion entropy S [Eq. (9)] in the ground state of the attractive Hubbard model for different structures, sizes, and band fillings of vanishing spin polarization ($N_\uparrow = N_\downarrow$). In (a), only first-NN hoppings $t_{ij} = -t < 0$ are taken into account: 1D rings having a number of sites $N_a = 6$ (circles), 10 (upright triangles), and 14 (squares), as well as 2D square lattices having $N_a = 2 \times 4$ (downright triangles) and $N_a = 3 \times 4$ (diamonds). The considered numbers of spin- σ fermions are $N_\sigma = 3$ (red), 4 (yellow), 5 (green), 6 (blue), and 7 (magenta). In (b), second-NN hoppings $t_{ij} = -t' = -t/2 < 0$ are included for the same structures and band fillings as in (a). In (c), results are shown for 1D rings with $N_a = 6$ (circles), 7 (squares), 8 (downright triangles), 10 (upright triangles), and 12 sites (diamonds) having strongly competing hopping integrals: first-NN hoppings $t_{ij} = -t < 0$ and second-NN hoppings $t_{ij} = -t' = 2t > 0$ (full symbols) as well as first-NN hoppings $t_{ij} = 0$ and second-NN hoppings $t_{ij} = -t' > 0$ (open symbols) for $N_\sigma = 2$ (red), 4 (green), and 6 (blue).

It is instructive to contrast the interaction-energy functional of the Hubbard model for attractive interactions $U < 0$, which we denote in the following by $W^-[\boldsymbol{\gamma}]$, with the corresponding functional of the repulsive case, which we denote by $W^+[\boldsymbol{\gamma}]$. Establishing any possible relation between W^+ and W^- would be helpful to guide the search for accurate approximations or to verify the validity of new ones. Consider the set $\Omega(\gamma_{ij\uparrow}, \gamma_{ij\downarrow})$ of all normalized pure states $|\Psi\rangle$ or, for that matter, mixed states $\hat{\rho}$, yielding the density matrix $\boldsymbol{\gamma}$, i.e., $\langle \Psi | \hat{c}_{i\sigma}^\dagger \hat{c}_{j\sigma} | \Psi \rangle = \gamma_{ij\sigma}$ for all $|\Psi\rangle \in \Omega(\gamma_{ij\uparrow}, \gamma_{ij\downarrow})$. This set is not empty since $\boldsymbol{\gamma}$ is physical, i.e., N representable. One may then identify the states $|\Psi_{\max}\rangle$ and $|\Psi_{\min}\rangle$ in $\Omega(\gamma_{ij\uparrow}, \gamma_{ij\downarrow})$ having the largest and smallest, respectively, total number of double occupations D . Let $D_{\max} = \langle \Psi_{\max} | \sum_i \hat{n}_{i\uparrow} \hat{n}_{i\downarrow} | \Psi_{\max} \rangle$ and $D_{\min} = \langle \Psi_{\min} | \sum_i \hat{n}_{i\uparrow} \hat{n}_{i\downarrow} | \Psi_{\min} \rangle$ be the corresponding maximum and minimum D within Ω , which are all functionals of $\boldsymbol{\gamma}$. There is no simple relation known to us between D_{\max} and D_{\min} for an arbitrary $\boldsymbol{\gamma}$. However, it is easy to conceive a bijective mapping of the set Ω onto an, in general, different set Ω^h in which $|\Psi_{\min}\rangle$ is assigned to $|\Psi_{\max}\rangle$ and vice versa. This is achieved by performing an electron-hole transformation on one of the spin components. For each $|\Psi\rangle \in \Omega$, one obtains its image $|\Psi^h\rangle \in \Omega^h$ by replacing the fermion creation operators $\hat{c}_{i\sigma}^\dagger$ by the hole operators $\hat{h}_{i\uparrow}^\dagger = \hat{c}_{i\uparrow}^\dagger$ and $\hat{h}_{i\downarrow}^\dagger = \hat{c}_{i\downarrow}$ and by replacing the vacuum state by the ket in which all down-spin orbitals are occupied. It follows that the density matrix $\boldsymbol{\gamma}^h$ of any state in Ω^h is given by

$$\gamma_{ij\uparrow}^h = \langle \Psi^h | \hat{c}_{i\uparrow}^\dagger \hat{c}_{j\uparrow} | \Psi^h \rangle = \langle \Psi^h | \hat{h}_{i\uparrow}^\dagger \hat{h}_{j\uparrow} | \Psi^h \rangle = \gamma_{ij\uparrow}, \quad (12)$$

$$\gamma_{ij\downarrow}^h = \langle \Psi^h | \hat{c}_{i\downarrow}^\dagger \hat{c}_{j\downarrow} | \Psi^h \rangle = \langle \Psi^h | \hat{h}_{i\downarrow}^\dagger \hat{h}_{j\downarrow} | \Psi^h \rangle = \delta_{ij} - \gamma_{ji\downarrow}. \quad (13)$$

Therefore, $\Omega^h \equiv \Omega(\gamma_{ij\uparrow}, \delta_{ij} - \gamma_{ji\downarrow})$. Moreover, the double-occupation operators transform as

$$\hat{n}_{i\uparrow} \hat{n}_{i\downarrow} = \hat{n}_{i\uparrow}^h (1 - \hat{n}_{i\downarrow}^h) = \hat{n}_{i\uparrow}^h - \hat{n}_{i\uparrow}^h \hat{n}_{i\downarrow}^h, \quad (14)$$

which implies that the total number of double occupations in $|\Psi^h\rangle$ is given by

$$\begin{aligned} D^h &= \langle \Psi^h | \sum_i \hat{n}_{i\uparrow} \hat{n}_{i\downarrow} | \Psi^h \rangle \\ &= \langle \Psi^h | \sum_i (\hat{n}_{i\uparrow}^h - \hat{n}_{i\uparrow}^h \hat{n}_{i\downarrow}^h) | \Psi^h \rangle = N_\uparrow - D, \end{aligned} \quad (15)$$

where D is the total number of double occupations in $|\Psi\rangle$. Since $N_\uparrow = \sum_i \gamma_{ii\uparrow}$ is the same for all $|\Psi\rangle$ and $|\Psi^h\rangle$, the change of sign in D means that the state $|\Psi_{\min}\rangle$ yielding the minimum number of double occupations D_{\min} in $\Omega(\gamma_{ij\uparrow}, \gamma_{ij\downarrow})$ is mapped into the state $|\Psi_{\max}^h\rangle$ yielding the maximum D_{\max}^h in $\Omega(\gamma_{ij\uparrow}, \delta_{ij} - \gamma_{ji\downarrow})$ and vice versa. One concludes that the interaction energy functionals W^- , corresponding to the attraction $U < 0$, and W^+ , corresponding to the repulsion $-U > 0$, are, in general, related by

$$W^-[\gamma_{ij\uparrow}, \delta_{ij} - \gamma_{ji\downarrow}] = U \sum_i \gamma_{ii\uparrow} + W^+[\gamma_{ij\uparrow}, \gamma_{ij\downarrow}], \quad (16)$$

where we have used that $W^-[\boldsymbol{\gamma}] = UD_{\max}[\boldsymbol{\gamma}]$ and $W^+[\boldsymbol{\gamma}] = -UD_{\min}[\boldsymbol{\gamma}]$ for $U < 0$. An analogous relation is obtained by exchanging the spin directions.

In periodic systems, we may focus on density matrices that comply with translational symmetry. Using that the eigenvectors of $\boldsymbol{\gamma}$ are Bloch states and, in particular, for single-band models, the interaction-energy functional can be regarded as a functional of the occupation-number distribution $\eta_{k\sigma}$. In this case, Eq. (16) implies

$$W^-[\eta_{k\uparrow}, 1 - \eta_{k\downarrow}] = U \sum_k \eta_{k\uparrow} + W^+[\eta_{k\uparrow}, \eta_{k\downarrow}]. \quad (17)$$

Notice that the approximations to W proposed in Eq. (11) for the attractive Hubbard model and in Ref. [34] for the repulsive case fulfill this exact relation in their common domain of validity, i.e., for $N_\uparrow = N_\downarrow = N_a/2$. Equations (16) and (17) can also be used to share and contrast any developments in the treatment of attractive and repulsive correlations in the Hubbard model within LDFT. One may furthermore note that the mapping between the kets $|\Psi\rangle$ and $|\Psi^h\rangle$ can be extended, using the same electron-hole transformation, to a mapping between the mixed states $\hat{\rho}$ and $\hat{\rho}^h$ which can be constructed by incoherently superposing them. This implies that the Eqs. (12), (13), and (15) relating $\gamma_{ij\sigma}$ and $\gamma_{ij\sigma}^h$ or D and D^h also hold when the averages are performed using the corresponding $\hat{\rho}$ and $\hat{\rho}^h$. Therefore, the Eqs. (16) and (17) connecting the attractive- and repulsive-interaction functionals also apply to the more general set of ensemble-representable density matrices $\gamma_{ij\sigma}$.

The ground-state energy E_0 and occupation-number distribution η^0 is obtained by minimizing the corresponding energy functional

$$E[\boldsymbol{\eta}] = \sum_{k\sigma} \varepsilon_k \eta_{k\sigma} + W[\boldsymbol{\eta}] \quad (18)$$

under the constraint $N_\sigma = \sum_k \eta_{k\sigma}$ on the number of spin- σ fermions. Let us recall that any IFE approximation of the form $W[\boldsymbol{\eta}] = W(S[\boldsymbol{\eta}])$ (i.e., one in which W depends on $\boldsymbol{\eta}$ through S) leads to ground-state occupation numbers $\eta_{k\sigma}^0$ which follow a Fermi-Dirac function with an effective temperature $T_{\text{eff}} = -\partial W/\partial S$ that depends only on U and N_σ [34]. The applications discussed in the following section show that the thus obtained Fermi-Dirac distributions are in most cases quite close to the exact ground-state occupation numbers of the attractive Hubbard model. Consequently, the linear IFE-approximation given by Eq. (11) is expected to yield a sound description of the most important ground-state observables in the complete range of interactions from weak to strong correlations.

IV. RESULTS

As a first application of the theory, we consider the 1D attractive Hubbard model and compare our results with exact numerical diagonalizations as well as with previous LDFT studies [18]. In Fig. 2, results are given for a number of relevant ground-state properties of a 14-site ring with NN hopping $t_{ij} = -t < 0$ and half-band filling, as functions of the interaction strength $|U|/t$. One observes that the ground-state energy E_0 decreases monotonously with increasing $|U|/t$,

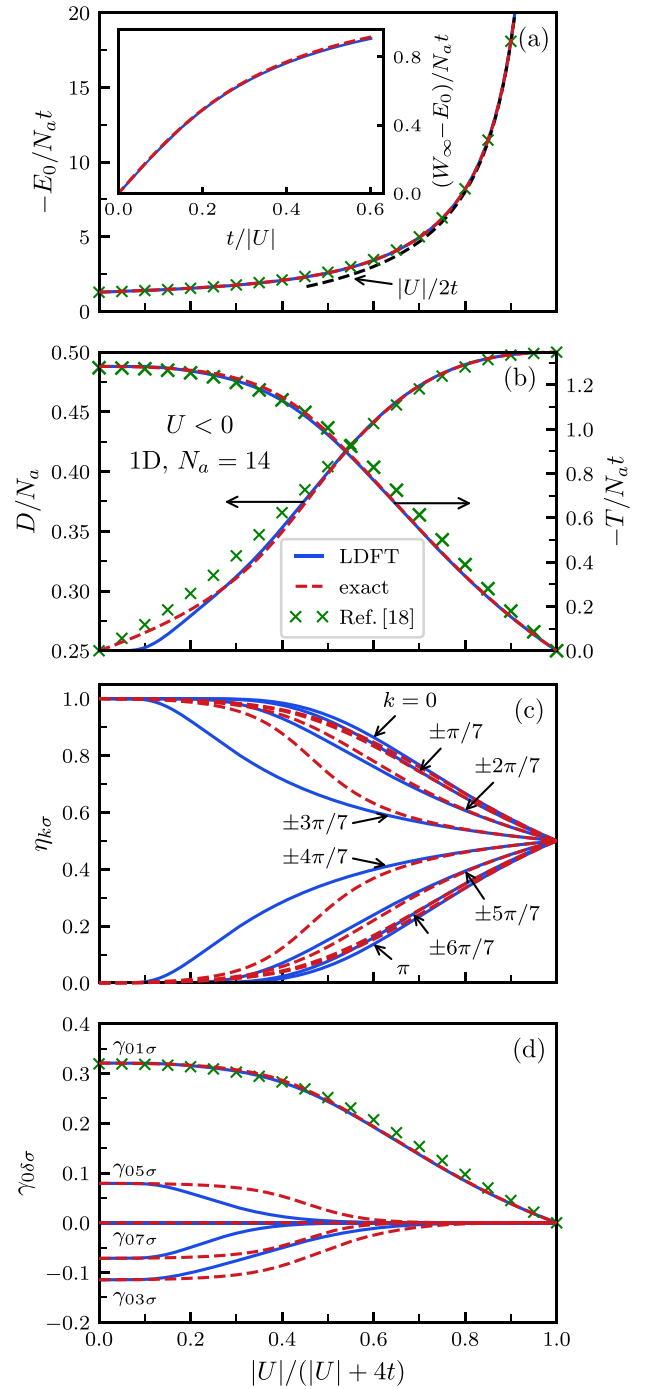


FIG. 2. Ground-state properties of the one-dimensional (1D) attractive Hubbard model on a 14-site ring with NN hoppings $t_{ij} = -t < 0$ and half-band filling as a function of the interaction strength $|U|/t$: (a) Ground-state energy E_0 , (b) average number of double occupations D and kinetic energy T , (c) natural-orbital occupation numbers $\eta_{k\uparrow} = \eta_{k\downarrow}$, and (d) single-particle density-matrix elements $\gamma_{0\delta\uparrow} = \gamma_{0\delta\downarrow}$ between site $i = 0$ and its δ th NN. The linear IFE approximation [Eq. (11), blue curves] is compared with exact numerical Lanczos diagonalizations (red dashed curves) and with the results of Ref. [18] whenever available (green crosses). The dashed black curve in (a) shows the strongly correlated limit of E_0 given by $W_\infty = -|U|N_a/2$. The inset of (a) highlights the energy gain $W_\infty - E_0$ in the strongly correlated limit ($t/|U| \ll 1$).

since the pairing energy overcompensates the kinetic-energy increase caused by the gradual fermion localization. The IFE results for E_0 follow the exact numerical calculations very closely in the complete range of the interaction strength $|U|/t$ [see Fig. 2(a)]. In the strongly correlated limit, $|U|/t \rightarrow \infty$, E_0 diverges tending to $W_\infty = -|U|N_a/2$ as $E_0 \simeq W_\infty - \alpha t^2/|U|$ with $\alpha > 0$, a fact which is highlighted in the inset of Fig. 2(a). The limit W_∞ represents the interaction energy of $N_a/2$ pairs ($N_\uparrow = N_\downarrow = N_a/2$) while the additional energy lowering $-\alpha t^2/|U|$ is a second-order perturbation correction in the hopping integrals consisting of the virtual breaking and recombination of pairs. The linear IFE approximation reproduces this behavior almost exactly with a leading coefficient $\alpha_{\text{IFE}} = 2.77$ which is only 0.7% smaller than the exact value $\alpha_{\text{ex}} = 2.79$ obtained from the Lanczos diagonalizations. Furthermore, it is interesting to observe that the accuracy of the IFE ansatz concerning E_0 is not the result of an important compensation of errors, since the average number of double occupations D and the kinetic energy T are very well reproduced separately, as shown in Fig. 2(b). Only in the weakly correlated limit ($|U|/t < 1$), we find that the present approximation underestimates the double occupations, which remain too close to the Hartree-Fock value $D_{\text{HF}} = N_a/4$. This can be ascribed mainly to deviations from linearity in $W(S)$ for nearly integer occupation numbers $\eta_{k\sigma} \simeq 0$ or 1, i.e., for small S , as can be seen in Fig. 1. Notice, however, that this does not affect the accuracy of the ground-state energy E_0 , since for weak interactions the kinetic energy, whose functional dependence is exactly known, largely dominates. In this interaction regime ($|U|/t \lesssim 0.5$), the scaling ansatz proposed in Ref. [18] yields a small overestimation of D and is, in general, closer to the exact results than the present calculations. However, as soon as the interaction and hopping integrals have comparable strengths ($|U|/t \gtrsim 1$), the linear IFE approximation clearly outperforms the previous real-space approach. This concerns not only the double occupations and the kinetic energy but also the NN bond order $\gamma_{01\sigma}$ shown in Fig. 2(d).

In Fig. 2(c), the Bloch-state occupation numbers $\eta_{k\sigma}$ are shown as functions of $|U|/t$. One observes that the present IFE approximation reproduces the crossover from weak to strong interactions qualitatively well. For $|U|/t \ll 1$, one obtains $\eta_{k\sigma} = 1$ for $|k| < \pi/2$ and $\eta_{k\sigma} = 0$ otherwise, as expected for weakly interacting fermions. As the interaction strength increases, charge fluctuations are progressively suppressed to favor local pairing. Consequently, $\eta_{k\sigma}$ decreases (increases) for $|k| < \pi/2$ ($|k| > \pi/2$) until $\eta_{k\sigma} \rightarrow 1/2$ for all $k\sigma$ in the strongly correlated limit. Quantitatively, the comparison with the exact results is in most cases remarkably good. Only for $|k| = 3\pi/7$ ($|k| = 4\pi/7$) at intermediate interaction strength, we find that the IFE ansatz underestimates (overestimates) $\eta_{k\sigma}$ significantly. This means that in these cases the excitations of electrons across the Fermi energy $\varepsilon_F = 0$, which are the result of correlations, are overestimated. The same behavior has already been observed in the repulsive case [34], which is not surprising since the attractive and repulsive Hubbard models are related by an electron-hole transformation [47]. In fact, it is easy to show that in the case of bipartite lattices and half-band filling the ground-state occupation numbers $\eta_{k\sigma}$ and the density matrix $\gamma_{ij\sigma}$ of the Hubbard model are independent of the sign of U . Knowing that the IFE approximation respects

this symmetry, the same trends are observed. From a local perspective, we observe that our approximation underestimates the delocalization of the electrons beyond first-NNs. Indeed, as shown in Fig. 2(d), $\gamma_{0\delta\sigma}$ tends to zero much faster than the exact result for $\delta = 3, 5$, and 7. They are significantly underestimated in absolute value for $1 \lesssim |U|/t \lesssim 6$. For even δ , we obtain $\gamma_{0\delta\sigma} = 0$ for all $|U|/t$ as required by the electron-hole symmetry. The $|U|/t$ dependence of $\gamma_{0\delta\sigma}$ shown in Fig. 2(d) coincides with the one observed in the repulsive model [34].

It is also interesting to assess the accuracy of the IFE ansatz away from half-band filling. In Fig. 3, exact and IFE results for several ground-state properties are shown for a 1D ring near 1/4-band filling, namely, $N_\sigma/N_a = 3/7$. The dependence of the ground-state properties on the interaction strength is found to be very similar to the half-filled case. These trends are remarkably well reproduced by the present approach in the complete range of interaction strength, from weak to strong correlations. Quantitatively, the IFE results are in some cases slightly more accurate than for $N_\sigma/N_a = 1$, for example, concerning the occupation numbers $\eta_{k\sigma}$ (compare Figs. 2 and 3). The most significant deviations are observed in the average number of double occupations D in the weakly correlated limit [Fig. 3(b)] where D is overestimated by about 15% for $|U| \rightarrow 0$. As discussed below, this discrepancy can be traced back to the presence of degeneracies at the Fermi level of the single-particle spectrum, which allows a reduction of D in the exact correlated state below the HF value, even for $U \rightarrow 0$. These inaccuracies are of little consequence for the other ground-state properties since the kinetic energy largely dominates in this limit.

The linear IFE approximation has also been applied to 2D lattices. In Fig. 4, results are shown for ground-state properties of the half-filled attractive Hubbard model on a 4×4 square-lattice cluster with NN hoppings and periodic boundary conditions ($N_\uparrow = N_\downarrow = 8$). The ground-state energy E_0 obtained with LDFT follows the exact results very closely in the complete range of the interaction strength $|U|/t$. The trends are similar to the 1D case. In particular, the strongly correlated limit, where $E_0 \simeq W_\infty - \alpha t^2/|U|$, is very well reproduced with a leading coefficient $\alpha_{\text{IFE}} = 5.55$ that is only 13% larger than the exact value $\alpha_{\text{ex}} = 4.81$ [see the inset of Fig. 4(a)].

The IFE results for the kinetic energy T [Fig. 4(b)] are also very good, although the differences with respect to the exact diagonalizations are more noticeable than in E_0 for intermediate $|U|/t$. Concerning the average number of double occupations D , one observes that any significant discrepancies between the IFE and exact results are restricted to the weakly correlated limit, namely, for $|U|/t \lesssim 2$ [see Fig. 4(b)]. These are most probably the consequence of the strong degeneracy of the single-particle spectrum of the 4×4 cluster at the partially filled Fermi level $\varepsilon_F = 0$. In fact, the Slater determinants constructed with different degenerate Bloch states having $\varepsilon_k = \varepsilon_F = 0$ can be linearly combined to enhance D beyond the Hartree-Fock value $D_{\text{HF}} = N_a/4$ without causing any kinetic-energy increase. Thus, the ground-state energy can be lowered in the limit of small $|U|/t$. Both the LDFT and exact calculations take advantage of this possibility and yield that all four Bloch states at the Fermi level are equally occupied with $\eta_{k\sigma} = 1/2$ [compare D_{IFE} and D_{ex} with $D_{\text{HF}} =$

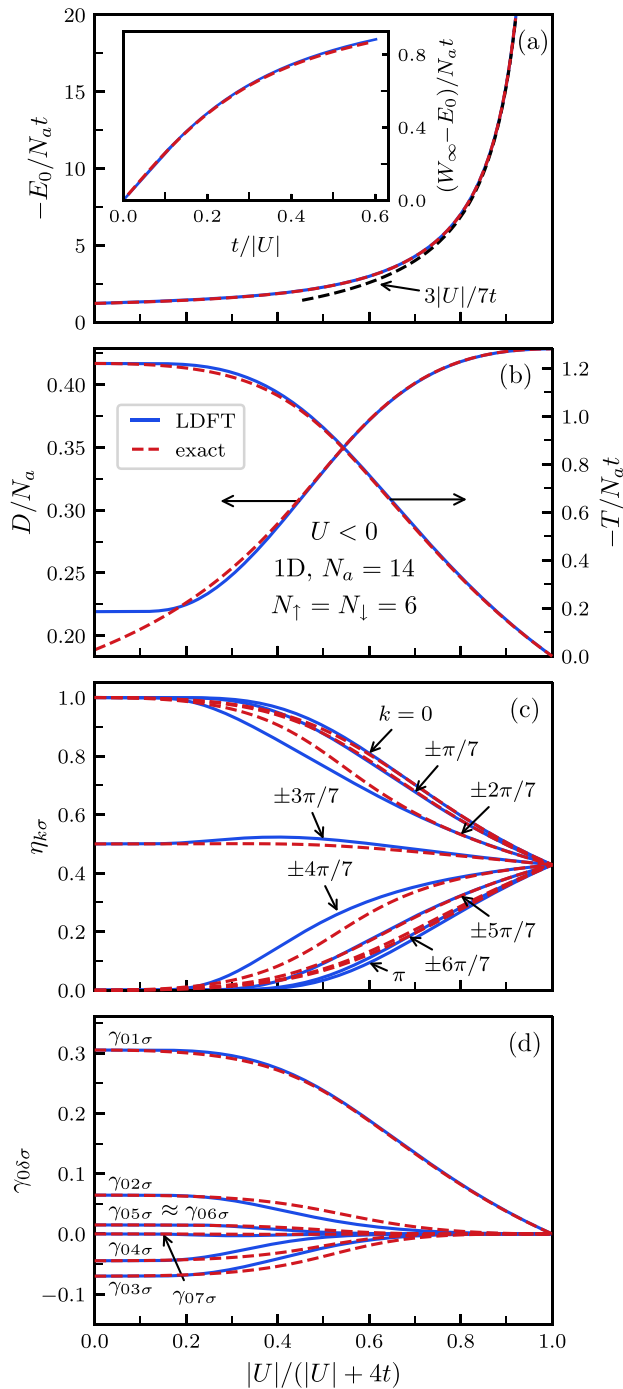


FIG. 3. Ground-state properties of the one-dimensional (1D) attractive Hubbard model on a 14-site ring with NN hoppings $t_{ij} = -t < 0$ and a band filling $N_\sigma/N_a = 3/7$ as a function of the interaction strength $|U|/t$. (a) Ground-state energy E_0 , (b) average number of double occupations D and kinetic energy T , (c) natural-orbital occupation numbers $\eta_{k\uparrow} = \eta_{k\downarrow}$, and (d) single-particle density-matrix elements $\gamma_{0\delta\uparrow} = \gamma_{0\delta\downarrow}$ between site $i = 0$ and its δ th NN. The linear IFE approximation [Eq. (11), blue curves] is compared with exact numerical Lanczos diagonalizations (red dashed curves). The dashed black curve in (a) shows the strongly correlated limit of E_0 given by $W_\infty = -|U|N_\sigma$. The inset of (a) highlights the energy gain $W_\infty - E_0$ in the strongly correlated limit ($t/|U| \ll 1$).

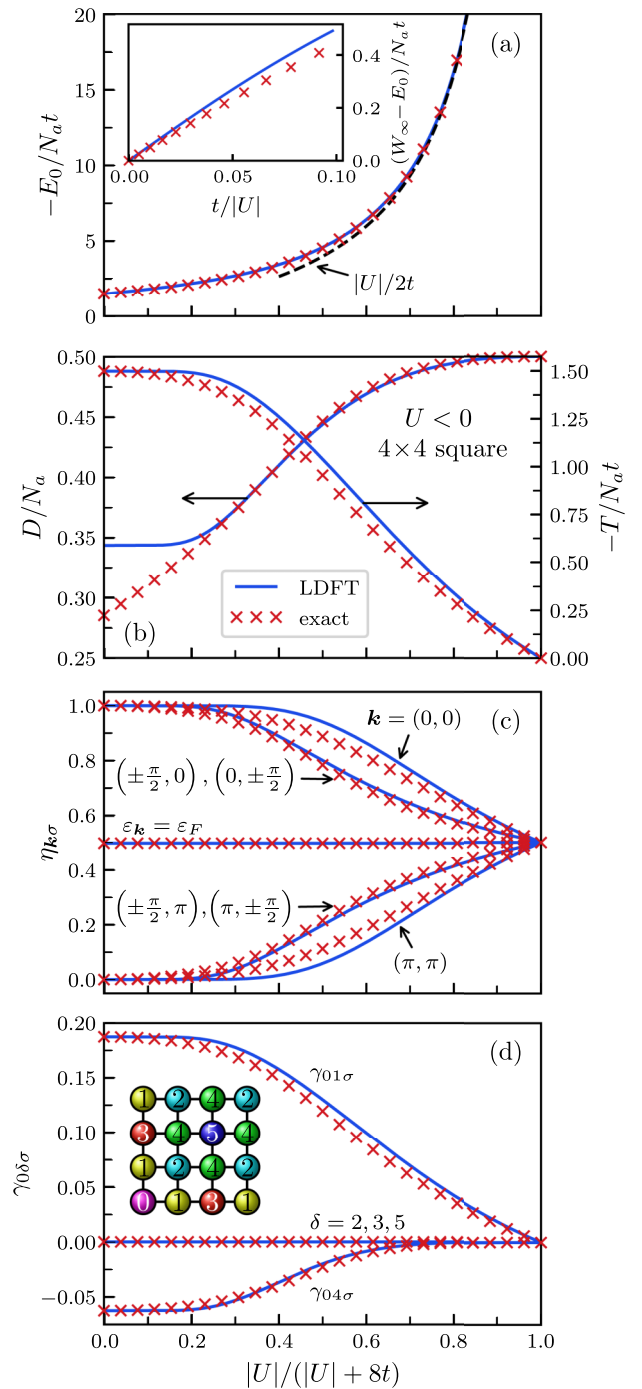


FIG. 4. Ground-state properties of the two-dimensional (2D) attractive Hubbard model on a 4×4 square-lattice cluster with NN hoppings $t_{ij} = -t < 0$, periodic boundary conditions and half-band filling ($N_\uparrow = N_\downarrow = 8$). The linear IFE approximation [Eq. (11)] (blue curves) is compared with exact numerical Lanczos diagonalizations (red crosses) as a function of the interaction strength $|U|/t$: (a) ground-state energy E_0 , (b) average number of double occupations D and kinetic energy T , (c) natural-orbital occupation numbers $\eta_{k\uparrow} = \eta_{k\downarrow}$, and (d) density-matrix elements $\gamma_{0\delta\uparrow} = \gamma_{0\delta\downarrow}$ between site $i = 0$ and its δ th NN, as labeled in the inset. The dashed black curve in (a) shows the strongly correlated limit of E_0 given by $W_\infty = -|U|N_a/2$. The inset of (a) highlights the ground-state energy gain $W_\infty - E_0$ in the strongly correlated limit ($t/|U| \ll 1$).

$N_a/4$ for $|U|/t \rightarrow 0$ in Fig. 4(b)]. However, the IFE approximation overestimates the ability of the system to enhance D by predicting $D_{\text{IFE}}/N_a \simeq 0.34$ whereas $D_{\text{ex}}/N_a \simeq 0.29$ for $|U|/t \rightarrow 0$. This overestimated value of D remains nearly constant at finite $|U|/t$ until the IFE result matches the exact one for $|U|/t \simeq 2$. Further increase of the interaction strength yields a monotonous increase of D in very good quantitative agreement with the exact results. This increase of D with increasing $|U|/t$ is accompanied with a decrease of the absolute value of the kinetic energy $|T|$ as the fermions begin to form pairs and localize ($T \leq 0$). Finally, as the fully localized state is approached for $|U|/t \rightarrow \infty$, only virtual pair-breaking remains possible and T vanishes proportionally to $-t^2/|U|$. As shown in Fig. 4(b), all these trends are very well reproduced by the IFE approximation to LDFT.

The dependence of the Bloch-state occupation numbers $\eta_{k\sigma}$ on $|U|/t$ is shown in Fig. 4(c). In the noninteracting limit, $\eta_{k\sigma} = 1$ ($\eta_{k\sigma} = 0$) for $\varepsilon_k < \varepsilon_F$ ($\varepsilon_k > \varepsilon_F$). The degenerate states at the Fermi level (i.e., for $\varepsilon_k = \varepsilon_F = 0$) have all $\eta_{k\sigma} = 1/2$ independent of $|U|/t$. As $|U|/t$ increases, one observes that $\eta_{k\sigma}$ decreases (increases) if $\varepsilon_k < \varepsilon_F$ ($\varepsilon_k > \varepsilon_F$), until $\eta_{k\sigma} = 1/2$ is reached for all $k\sigma$ in the strongly correlated limit, which corresponds to a fully localized state. The occupation numbers $\eta_{k\sigma}$ obtained within the IFE approximation are remarkably accurate for all $k\sigma$ in the complete range from weak to strong interactions. Furthermore, note that the approximation respects all the point-group symmetries of $\eta_{k\sigma}$ in the reciprocal space, since they are inherited from the corresponding symmetries of the dispersion relation ε_k .

The very good accuracy of the Bloch-state occupation numbers $\eta_{k\sigma}$ anticipates a comparably good accuracy of the SPDM elements $\gamma_{ij\sigma}$, which are shown in Fig. 4(d). One observes how the nonvanishing $\gamma_{01\sigma}$ and $\gamma_{04\sigma}$ between first and fourth neighbors are gradually suppressed as the interaction strength $|U|/t$ increases. This reflects the correlation-induced suppression of charge fluctuations and the transition to a localized state as the fermions condense into localized pairs. One may furthermore notice that the charge fluctuations at longer distances $|\gamma_{04\sigma}|$ are suppressed faster than the fluctuations $\gamma_{01\sigma}$ between NNs, a trend which is reproduced by the proposed IFE approximation.

In Fig. 5, the effects of second-NN hoppings on the ground-state properties of the square lattice are investigated by considering a 4×4 cluster with NN hopping $t_{ij} = -t < 0$ and second-NN hoppings $t_{ij} = -t' = -t/2$. Comparison with Fig. 4 shows that the dependencies of the kinetic, interaction, and total energies as functions of $|U|/t$ are not strongly affected by breaking the bipartite character of the NN square lattice. More significant changes are observed, as expected, in the density-matrix elements $\gamma_{ij\sigma}$ and in the occupation numbers $\eta_{k\sigma}$ of the Bloch states [see Figs. 5(c) and 5(d)]. The accuracy of the linear IFE ansatz remains, in general, very good when $t' = t/2$ is introduced, for example, concerning the ground-state energy E_0 . This is particularly remarkable in the crossover region from weak to strong correlations ($1 \lesssim |U|/t \lesssim 10$) where the interplay between the fermion delocalization, driven by the hybridizations, and the tendency to pair formation and localization is far from trivial. As in the bipartite case ($t' = 0$, Fig. 4) the asymptotic

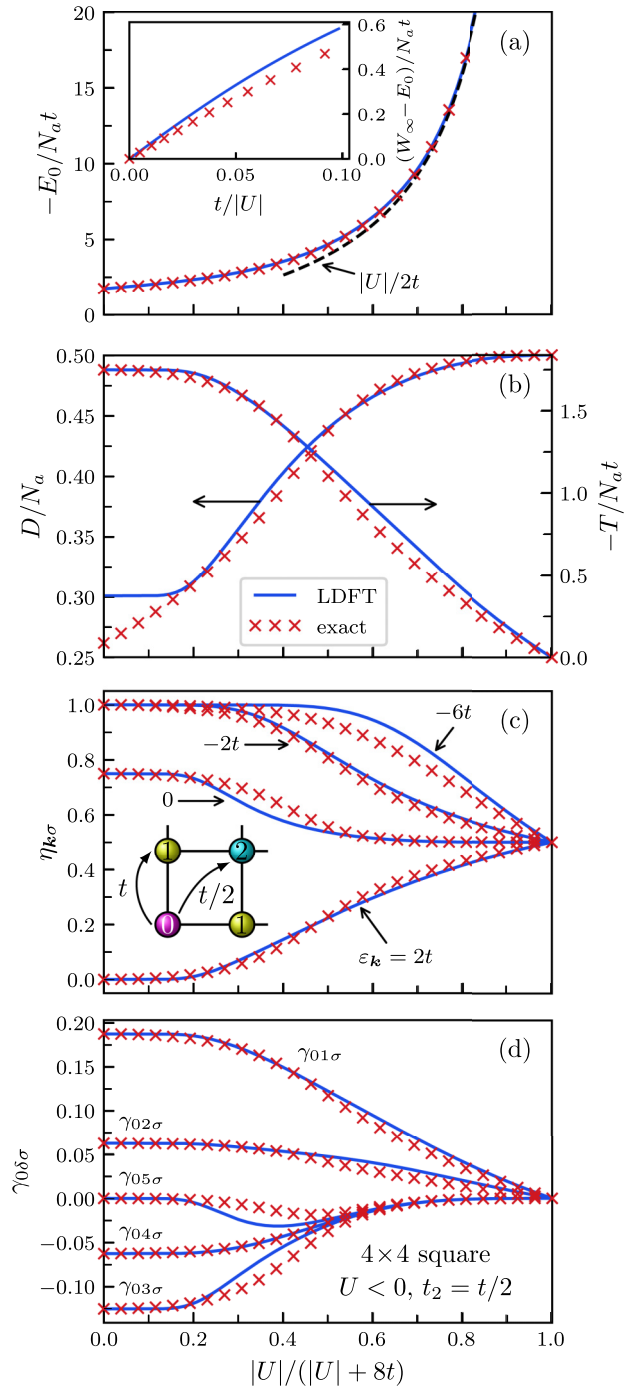


FIG. 5. Ground-state properties of the half-filled attractive 2D Hubbard model on a 4×4 periodic square lattice with NN hoppings $t_{ij} = -t < 0$ and second-NN hoppings $t_{ij} = -t' = -t/2$. The linear IFE approximation (blue curves) is compared with exact numerical Lanczos diagonalizations (red crosses) as a function of the interaction strength $|U|/t$: (a) ground-state energy E_0 , (b) average number of double occupations D and kinetic energy T , (c) natural-orbital occupation numbers $\eta_{k\uparrow} = \eta_{k\downarrow}$, and (d) density-matrix elements $\gamma_{0\delta\uparrow} = \gamma_{0\delta\downarrow}$ between site $i = 0$ and its δ th NN, as labeled in the inset of Fig. 4 (d). The dashed black curve in (a) shows the strongly correlated limit of E_0 given by $W_\infty = -|U|N_a/2$. The inset of (a) highlights the ground-state energy gain $W_\infty - E_0$ in the strongly correlated limit ($t/|U| \ll 1$).

behavior $E_0 \simeq -|U|N_a/2 - \alpha t^2/|U|$ in the strongly correlated limit is qualitatively reproduced as highlighted in the inset of Fig. 5(a). Quantitatively, the coefficient $\alpha_{\text{IFE}} = 6.93$ is larger than in the case with only first-NN hoppings ($\alpha_{\text{IFE}} = 5.55$ for $t' = 0$) which implies an increased stabilization due to virtual pair breaking. This enhancement of α is in qualitative agreement with the trends observed in the exact diagonalizations, which yield $\alpha_{\text{ex}} = 5.65$ for $t' = t/2$ and $\alpha_{\text{ex}} = 4.81$ for $t' = 0$. However, in all cases the IFE functional results in an overestimation of about 20% of the binding energy.

The average number of ground-state double occupations D and the kinetic energy T show a dependence on $|U|/t$ that is very similar to the case where only NN hoppings are taken into account [compare (b) and (c) of Figs. 4 and 5]. The exact diagonalizations show that for $|U|/t \rightarrow 0$, the second-NN hoppings $t' = t/2$ cause a 17% lowering of T at the expense of an 8% decrease of D . Since the kinetic-energy functional is exact in LDFT, the above-mentioned kinetic-energy lowering is exactly reproduced by the IFE approximation. However, D is clearly overestimated in the weakly interacting regime. This is probably related to the degeneracies at the Fermi level of the single-particle spectrum, as in the $t' = 0$ case. Despite the overestimation, the IFE calculations yield a 13% reduction of D for $|U|/t \rightarrow 0$ due to the second-NN hoppings $t' = t/2$, which is in good qualitative agreement with the 8% reduction obtained in the corresponding exact solution. The difficulties found at weak interactions disappear for $|U|/t \gtrsim 2$, where LDFT recovers its usual very good accuracy.

In Fig. 5(c), results are shown for the Bloch-state occupation numbers $\eta_{k\sigma}$. As expected, the $\eta_{k\sigma}$ which are larger (smaller) than $1/2$ decrease (increase) as $|U|/t$ increases, reaching the common limit $\eta_{k\sigma} = 1/2$ for all \mathbf{k} in the localized state when $|U|/t \rightarrow \infty$. An interesting difference with respect to the $t' = 0$ case is observed at the Fermi energy where $t' = t/2$ reduces the degeneracy from 6 to 4. Since ε_F is occupied by three fermions, we have $\eta_{k\sigma} = 3/4$ in the weakly correlated limit. Consequently, these occupation numbers decrease with increasing $|U|/t$, in contrast to the bipartite lattice [see Figs. 4(c) and 5(c)]. Comparison with the exact diagonalizations shows that the IFE approximation reproduces all the Bloch-state occupation numbers with very good accuracy from weak to strong correlations. Notice, however, that $\eta_{k\sigma}$ is somewhat overestimated for $\mathbf{k} = (0, 0)$ ($\varepsilon_{\mathbf{k}} = -6t$) and intermediate $|U|/t$, which incidentally explains the overestimation of $|T|$ in this range. For example, for $|U|/t = 15$, we find that $\eta_{k\sigma}$ is overestimated by 8.7% for $\mathbf{k} = (0, 0)$ and $|T|$ is overestimated by about 17% [see Figs. 5(b) and 5(c)].

The density-matrix elements $\gamma_{0\delta\sigma}$ between the lattice site $i = 0$ and its δ th NN are given in Fig. 5(d) as a function of $|U|/t$. The hopping integrals t' between second-NNs introduce hybridizations between sites belonging to the same sublattice (e.g., between $i = 0$ and $i = 2, 3$, and 5) which are absent in the bipartite case [see the inset of Fig. 4(d)]. As a result, $\gamma_{0\delta\sigma}$ is no longer zero for $\delta = 2, 3$, and 5. In particular, $\gamma_{05\sigma}$ shows a remarkable nonmonotonous behavior with a minimum at $|U|/t \simeq 8$. This is qualitatively reproduced by the IFE ansatz, although somewhat exaggerated and slightly

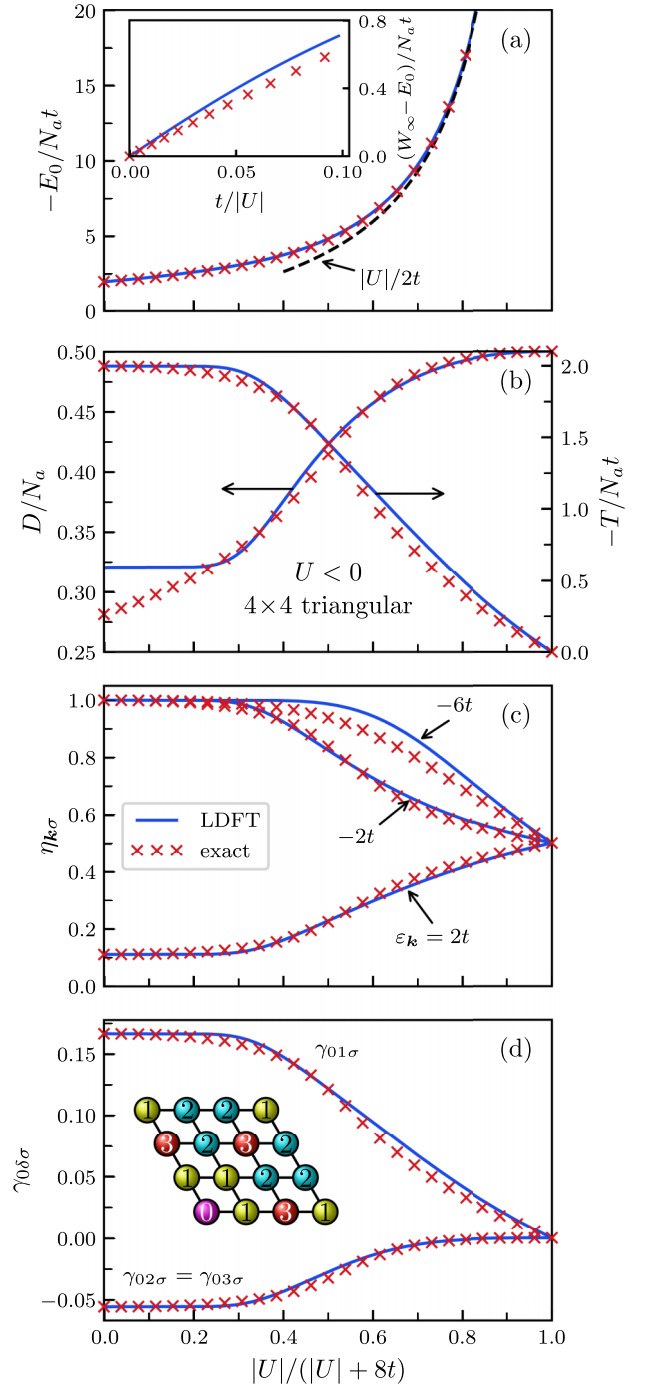


FIG. 6. Ground-state properties of the two-dimensional (2D) attractive Hubbard model on a 4×4 triangular-lattice cluster with NN hoppings $t_{ij} = -t < 0$, periodic boundary conditions, and half-band filling ($N_\uparrow = N_\downarrow = 8$). The linear IFE approximation (blue curves) is compared with exact numerical Lanczos diagonalizations (red crosses) as a function of the interaction strength $|U|/t$: (a) ground-state energy E_0 , (b) average number of double occupations D and kinetic energy T , (c) natural-orbital occupation numbers $\eta_{k\uparrow} = \eta_{k\downarrow}$, and (d) density-matrix elements $\gamma_{0\delta\uparrow} = \gamma_{0\delta\downarrow}$ between site $i = 0$ and its δ th NN, as labeled in the inset. The dashed black curve in (a) shows the strongly correlated limit of E_0 given by $W_\infty = -|U|N_a/2$. The inset of (a) highlights the ground-state energy gain $W_\infty - E_0$ in the strongly correlated limit ($t/U \ll 1$).

shifted to smaller $|U|/t$. This behavior might be related to the rapid decrease of $\eta_{k\sigma}$ for $\varepsilon_k = \varepsilon_F = 0$ in the same range of $|U|/t$ [see Fig. 5(c)].

As an example of a nonbipartite lattice with triangular NN loops, we consider the 2D triangular lattice, which is modeled by a 4×4 cluster with periodic boundary conditions [see the inset of Fig. 6 (d)]. As in previous cases, the comparison with exact results shows that the IFE approximation gives a very accurate account of the ground-state energy E_0 for all $|U|/t$ [see Fig. 6(a)]. In the limit of strong correlations, in particular, we obtain the right asymptotic dependence $E_0 \simeq -|U|N_a/2 - \alpha t^2/|U|$ with $\alpha_{\text{IFE}} = 8.32$. This should be compared with the exact leading correction having $\alpha_{\text{ex}} = 6.73$ as shown in the inset of Fig. 6(a). Also, the kinetic energy T is very well reproduced, which implies that the accuracy of E_0 is not the result of strong compensation of errors in the kinetic and interaction contributions [see Fig. 6(b)]. Only the average number of double occupations in the weakly interacting regime ($|U|/t \lesssim 3$) shows, as in previous cases, a significant overestimation which can be traced back to the degeneracies in the single-particle spectrum at the Fermi level.

The Bloch-state occupation numbers $\eta_{k\sigma}$ given in Fig. 6(c) display the familiar trend as a function of $|U|/t$ which ends up in localization in the strongly correlated limit (i.e., $\eta_{k\sigma} = 1/2$ for all $k\sigma$ at $|U|/t \rightarrow \infty$). At half-band filling, the Fermi energy ε_F is given by the highest single-particle level $\varepsilon_k = 2t$, which is ninefold degenerate. For $|U|/t = 0$, one thus finds $\eta_{k\sigma} = 1/9$ for all the degenerate Bloch states since ε_F is occupied by only one fermion per spin. The comparison with the exact numerical results shows that the IFE approximation yields a very accurate occupation-number distribution $\eta_{k\sigma}$ for all $|U|/t$. Only the occupation of the lowest-lying Bloch state having $\mathbf{k} = (0, 0)$ and $\varepsilon_k = -6t$ is somewhat overestimated for intermediate values $|U|/t$. Finally, the very good results for $\eta_{k\sigma}$ also explain the high accuracy of the IFE approximation for the density-matrix elements $\gamma_{0\delta\sigma}$ shown in Fig. 6(d).

V. CONCLUSION

An interaction-energy functional has been developed to investigate the ground state of the Hubbard model with attractive pairing interactions in the framework of LDFT. Our approach takes a reciprocal \mathbf{k} -space perspective and exploits an approximate functional relation between the interaction energy $W[\eta]$ of the Hubbard model corresponding to the Bloch-state occupation-number distribution $\eta_{k\sigma}$ and the entropy $S[\eta]$ of a system of noninteracting fermions having the same occupation numbers $\eta_{k\sigma}$. This has opened up a unique perspective to the ground-state problem of periodic systems, which takes into account the dependence of the central interaction-energy functional $W[\gamma]$ on all elements of the SPDM γ and thus leverages the universality of LDFT. The relation between $W[\eta]$ and $S[\eta]$ has been shown to be approximately linear for a wide range of ground-state representable occupation-number distributions $\eta_{k\sigma}$. On this basis, a simple and very effective approximation to $W[\eta]$ has been inferred. The flexibility and efficacy of this linear IFE ansatz has been demonstrated in applications to the attractive 1D and 2D Hubbard model on bipartite and nonbipartite lattices. Comparisons with exact numerical Lanczos diagonalizations on finite clusters have demonstrated the remarkable accuracy of this approximation in the complete attractive-interaction range from weak to strong correlations. The present formulation, which incorporates a statistical or information-theory perspective, turns out to open a useful alternative route in the search for increasingly accurate and more broadly applicable approximations to the interaction energy of strongly correlated systems in the framework of LDFT.

ACKNOWLEDGMENTS

Helpful discussions with W. Töws are gratefully acknowledged. Computer resources were provided by the IT Service Center of the University of Kassel and by the Center for Scientific Computing of the Goethe University of Frankfurt.

- [1] E. Dagotto, Correlated electrons in high-temperature superconductors, *Rev. Mod. Phys.* **66**, 763 (1994).
- [2] J. G. Bednorz and K. A. Müller, Possible high- T_c superconductivity in the Ba-La-Cu-O system, *Z. Phys. B* **64**, 189 (1986).
- [3] J. Bardeen, L. N. Cooper, and J. R. Schrieffer, Theory of superconductivity, *Phys. Rev.* **108**, 1175 (1957).
- [4] N. Bickers, D. Scalapino, and R. Scalettar, CDW and SDW mediated pairing interactions, *Int. J. Mod. Phys. B* **01**, 687 (1987).
- [5] G. Baskaran and P. W. Anderson, Gauge theory of high-temperature superconductors and strongly correlated Fermi systems, *Phys. Rev. B* **37**, 580 (1988).
- [6] G. Kotliar and J. Liu, Superexchange mechanism and d-wave superconductivity, *Phys. Rev. B* **38**, 5142 (1988).
- [7] J. R. Schrieffer, X. G. Wen, and S. C. Zhang, Dynamic spin fluctuations and the bag mechanism of high- T_c superconductivity, *Phys. Rev. B* **39**, 11663 (1989).
- [8] A. Kampf and J. R. Schrieffer, Pseudogaps and the spin-bag approach to high- T_c superconductivity, *Phys. Rev. B* **41**, 6399 (1990).
- [9] P. W. Anderson, The Theory of High T_c Superconductivity, in *High-Temperature Superconductivity*, edited by J. Ashkenazi, S. E. Barnes, F. Zuo, G. C. Vezzoli, and B. M. Klein (Springer, New York, NY, 1991), pp. 1–6.
- [10] P. W. Anderson and K. S. Bedell, The theory of superconductivity in the high- T_c cuprates, *Phys. Today* **51**(7), 64 (1998).
- [11] J. Hubbard, Electron correlations in narrow energy bands, *Proc. R. Soc. London A* **276**, 238 (1963).
- [12] J. Kanamori, Electron correlation and ferromagnetism of transition metals, *Prog. Theor. Phys.* **30**, 275 (1963).
- [13] M. C. Gutzwiller, Effect of Correlation on the Ferromagnetism of Transition Metals, *Phys. Rev. Lett.* **10**, 159 (1963).
- [14] J. E. Hirsch and D. J. Scalapino, Excitonic mechanism for superconductivity in a quasi-one-dimensional system, *Phys. Rev. B* **32**, 117 (1985).
- [15] J. E. Hirsch and D. J. Scalapino, Enhanced Superconductivity in Quasi Two-Dimensional Systems, *Phys. Rev. Lett.* **56**, 2732 (1986).
- [16] R. T. Scalettar, E. Y. Loh, J. E. Gubernatis, A. Moreo, S. R. White, D. J. Scalapino, R. L. Sugar, and E. Dagotto, Phase

- Diagram of the Two-Dimensional Negative- U Hubbard Model, *Phys. Rev. Lett.* **62**, 1407 (1989).
- [17] T. Paiva, R. R. dos Santos, R. T. Scalettar, and P. J. H. Denteneer, Critical temperature for the two-dimensional attractive Hubbard model, *Phys. Rev. B* **69**, 184501 (2004).
- [18] M. Saubanère and G. M. Pastor, Lattice density-functional theory of the attractive Hubbard model, *Phys. Rev. B* **90**, 125128 (2014).
- [19] E. C. Stoner, Collective electron ferromagnetism, *Proc. R. Soc. London A* **165**, 372 (1938).
- [20] P. W. Anderson, Localized magnetic states in metals, *Phys. Rev.* **124**, 41 (1961).
- [21] J. Kondo, Resistance minimum in dilute magnetic alloys, *Prog. Theor. Phys.* **32**, 37 (1964).
- [22] R. Micnas, J. Ranninger, and S. Robaszkiewicz, Superconductivity in narrow-band systems with local nonretarded attractive interactions, *Rev. Mod. Phys.* **62**, 113 (1990).
- [23] F. Marsiglio, Evaluation of the BCS approximation for the attractive Hubbard model in one dimension, *Phys. Rev. B* **55**, 575 (1997).
- [24] K. Tanaka and F. Marsiglio, Even-odd and super-even effects in the attractive Hubbard model, *Phys. Rev. B* **60**, 3508 (1999).
- [25] N. Salwen, S. A. Sheets, and S. R. Cotanch, BCS and attractive Hubbard model comparative study, *Phys. Rev. B* **70**, 064511 (2004).
- [26] J.-H. Hu, J.-J. Wang, G. Xianlong, M. Okumura, R. Igarashi, S. Yamada, and M. Machida, Ground-state properties of the one-dimensional attractive Hubbard model with confinement: A comparative study, *Phys. Rev. B* **82**, 014202 (2010).
- [27] C. Schilling, Communication: Relating the pure and ensemble density matrix functional, *J. Chem. Phys.* **149**, 231102 (2018).
- [28] C. Schilling and R. Schilling, Diverging Exchange Force and Form of the Exact Density Matrix Functional, *Phys. Rev. Lett.* **122**, 013001 (2019).
- [29] J. Schmidt, C. L. Benavides-Riveros, and M. A. L. Marques, Reduced density matrix functional theory for superconductors, *Phys. Rev. B* **99**, 224502 (2019).
- [30] C. L. Benavides-Riveros, J. Wolff, M. A. L. Marques, and C. Schilling, Reduced Density Matrix Functional Theory for Bosons, *Phys. Rev. Lett.* **124**, 180603 (2020).
- [31] J. Schmidt, M. Fadel, and C. L. Benavides-Riveros, Machine learning universal bosonic functionals, *Phys. Rev. Res.* **3**, L032063 (2021).
- [32] P. Hohenberg and W. Kohn, Inhomogeneous electron gas, *Phys. Rev.* **136**, B864 (1964).
- [33] R. G. Parr and W. Yang, *Density-Functional Theory of Atoms and Molecules* (Oxford University Press, New York, 1995).
- [34] T. S. Müller, W. Töws, and G. M. Pastor, Exploiting the links between ground-state correlations and independent-fermion entropy in the Hubbard model, *Phys. Rev. B* **98**, 045135 (2018).
- [35] R. López-Sandoval and G. M. Pastor, Density-matrix functional theory of the Hubbard model: An exact numerical study, *Phys. Rev. B* **61**, 1764 (2000).
- [36] W. Töws, M. Saubanère, and G. M. Pastor, Density-matrix functional theory of strongly correlated fermions on lattice models and minimal-basis Hamiltonians, *Theor. Chem. Acc.* **133**, 1422 (2014).
- [37] W. Töws and G. M. Pastor, Lattice density functional theory of the single-impurity Anderson model: Development and applications, *Phys. Rev. B* **83**, 235101 (2011).
- [38] M. Levy, Electron densities in search of Hamiltonians, *Phys. Rev. A* **26**, 1200 (1982).
- [39] E. H. Lieb, Density functionals for Coulomb systems, *Int. J. Quantum Chem.* **24**, 243 (1983).
- [40] S. M. Valone, Consequences of extending 1-matrix energy functionals from pure-state representable to all ensemble representable 1 matrices, *J. Chem. Phys.* **73**, 1344 (1980).
- [41] S. M. Valone, A one-to-one mapping between one-particle densities and some n -particle ensembles, *J. Chem. Phys.* **73**, 4653 (1980).
- [42] The domain of definition of $W[\boldsymbol{\gamma}]$ comprises not only density matrices which can be derived from some ground state of the Hubbard model (i.e., the so-called ground-state representable $\boldsymbol{\gamma}$) but the much broader set of ensemble-representable density matrices, which can be derived from an arbitrary mixed state $\hat{\rho}$. The necessary and sufficient condition for a density matrix to be ensemble representable is simply that all its eigenvalues $\eta_{k\sigma}$ are comprised between zero and one.
- [43] D. M. Collins, Entropy maximizations on electron density, *Z. Naturforsch. Teil A* **48**, 68 (1993).
- [44] In Ref. [43], the importance of the growing statistical uncertainty in the occupation-number distribution resulting from increasing correlations has been clearly identified. The arguments presented here to derive Eq. (9) in the weakly correlated limit are very similar to those formulated in Collins' work. However, Eq. (9) is profoundly different physically from the information entropy $S = -\sum_k \eta_k \ln(\eta_k)$ considered in Ref. [43]. Equation (9) represents the entropy of a many-body system of noninteracting fermions having the same occupation-number distribution $\eta_{k\sigma}$ as the interacting system under consideration. Thus, the fermionic character of the particles is correctly taken into account and the fundamental electron-hole symmetry of $W[\boldsymbol{\eta}]$ is respected, which does not hold for Collins' conjecture.
- [45] N. Flores-Gallegos, Informational energy as a measure of electron correlation, *Chem. Phys. Lett.* **666**, 62 (2016).
- [46] Y. Wang, P. J. Knowles, and J. Wang, Information entropy as a measure of the correlation energy associated with the cumulant, *Phys. Rev. A* **103**, 062808 (2021).
- [47] The electron-hole transformation relating positive- U and negative- U Hubbard models is obtained by introducing the following hole-annihilation operators: $\hat{h}_{i\uparrow} = \hat{c}_{i\uparrow}$ and $\hat{h}_{i\downarrow} = \hat{c}_{i\downarrow}^\dagger$. It implies a change of sign in the down-spin hopping integrals and therefore leaves \hat{H} invariant only for bipartite lattices, in which case one sets $\hat{h}_{i\downarrow} = -\hat{c}_{i\downarrow}^\dagger$ for i belonging to one of the two sublattices. In addition, an irrelevant shift of the total energy is obtained. Notice that if $\Delta S_z = N_\downarrow - N_\uparrow/2 \neq 0$ a change in the total spin-polarization $S_z^{(h)} = S_z + \Delta S_z$ is involved.